Journal of Power Sources 262 (2014) 303–309

Contents lists available at ScienceDirect

Journal of Power Sources

journal homepage: www.elsevier.com/locate/jpowsour

Effect of methylene methanedisulfonate as an additive on the cycling performance of $LiMn_2O_4$ cathode at elevated temperature

Tao Huang, Maoxiang Wu*, Wenguo Wang, Ying Pan, Guihuang Fang

State Key Laboratory of Structural Chemistry, Fujian Institute of Research on the Structure of Matter, Chinese Academy of Sciences, Fuzhou 350002, PR China

HIGHLIGHTS

- MMDS used as additive to improve cycling performance of the $LiMn_2O_4$/Li cell at 55 °C.
- MMDS participated in the formation of SEI on the surface of electrode.
- Sulfur-containing species is the main component of the SEI formed by MMDS.

ARTICLE INFO

Article history:
Received 19 December 2013
Received in revised form
7 March 2014
Accepted 26 March 2014
Available online 13 April 2014

Keywords:
Lithium–ion battery
Electrolyte additive
Solid electrolyte interphase layer
Methylene methanedisulfonate

ABSTRACT

In order to overcome the capacity fading of $LiMn_2O_4$ cathode lithium–ion batteries (LIBs) cycled at elevated temperature, methylene methanedisulfonate (MMDS) is newly evaluated as an electrolyte additive. With the addition of 0.5 wt.% MMDS into the electrolyte (1.0 M $LiPF_6$-EC/DMC/EMC), the capacity retention of the $LiMn_2O_4$/Li cell cycled at 55 °C is significantly increased from 51.6% to 72.8% after 200 cycles, showing the promising prospect in the electrolyte. In addition, the results of electrochemical impedance spectroscopy (EIS), X-ray photoelectron spectroscopy (XPS), scanning electron microscope (SEM) and transmission electron microscopy (TEM) demonstrate that a thin and good conductive film can be formed on the $LiMn_2O_4$ surface ascribed to MMDS additive, which resulting the suppression of the electrolyte oxidized decomposition, the improvement of SEI conductivity and a good ability of Li^+ migration.

1. Introduction

$LiMn_2O_4$ becomes the promising cathode material for commercial usage due to the low cost, good safety performance and benign to environment [1,2]. However, the cells used $LiMn_2O_4$ spinel as a cathode material have been known to cause severe capacity fading on charge–discharge cycling or storage at high temperature, especially above 50 °C.

The reasons for capacity fading are the following: Mn dissolution, Jahn–Teller effect, and electrolyte decomposition [3–8]. The erosion to $LiMn_2O_4$ of the electrolyte is the important reason for capacity fading and poor cycling performance [5–8]. In order to suppress Mn^{2+} dissolution, many intensive investigations have been carried out on the $LiMn_2O_4$. Using an electrolyte additive is one of the most economical and effective methods to solve these problems. Zhang reported [9] that the amount of an additive in the electrolyte is no more than 5% either by weight or by volume while its presence significantly improves the cycling performance of Lithium ion batteries. Some additives have been reported to facilitate formation of the cathode electrolyte interphase (SEI) on the surface of the $LiMn_2O_4$ electrode at high temperature, which protects the cathode material from dissolution and electrolyte decomposition, therefore, improving the cycling performance of $LiMn_2O_4$ in a sense. Sun et al. [10] reported tris(pentafluorophenyl) borane (TPFPB) can reduce production of electrolyte decomposition residues. The $LiMn_2O_4$/Li battery with the $LiPF_6$-based electrolyte containing 0.1 M TPFPB additive reduced capacity fading and enhanced cycling performance at 55 °C than the battery without additive. Park et al. [11] used fluoroethylene carbonate (FEC) as an electrolyte additive. The $LiMn_2O_4$/graphite LIBs with $LiPF_6$-based electrolyte containing 2 wt.% FEC improved the capacity retention at 60 °C. Li et al. [12] added 0.1 wt.% heptamethyldisilazane to $LiPF_6$-based electrolyte. It improves the stability of the electrolyte, storage performance and cycling performance of $LiMn_2O_4$/graphite LIBs batteries. Liu et al. [13] discussed the effects of the tris(-trimethylsilyl) borate (TMSB) on the $LiMn_2O_4$ electrode. With

* Corresponding author. Tel.: +86 591 8370 4985; fax: +86 591 8375 3263.
E-mail address: mxwu@fjirsm.ac.cn (M. Wu).

http://dx.doi.org/10.1016/j.jpowsour.2014.03.129
0378-7753/

0.5 wt.% TMSB addition into the $LiPF_6$-based electrolyte, the capacity retention is significantly improved at both room temperature and 55 °C.

Methylene methanedisulfonate (MMDS) has been reported as an electrolyte additive for the formation of a good cathode layer on the $LiCoO_2$ electrode at high voltage [14]. In order to improve cycling performance of $LiMn_2O_4$/Li cell at 55 °C, MMDS was chosen as an electrolyte additive which is facilitate formation of the solid electrolyte interphase and added to a 1.0 M $LiPF_6$-EC/DMC/EMC(1:1:1, wt.%) electrolyte to investigate its effects on the electrochemical performance of $LiMn_2O_4$/Li cell in this paper.

2. Experimental

2.1. Synthesis of methylene methanedisulfonate

Methanedisulfonic acid (100 g, 0.53 mol), phosphoric anhydride (156 g, 0.62 mol) and part of paraformaldehyde were placed in a 500 ml 3-neck flask under argon, stirred at 90–120 °C. The remaining paraformaldehyde (total 18.7 g, 0.62 mol) was added dropwise over 1.5 h, and then the reaction mixture was stirred under 100–120 °C for continued 2 h. The resulting mixture was then cooled to room temperature, added ice deionized water and stirred, the pale solid was separated out. The solid was washed 3 times with ice deionized water, yielding small pale crystals. The crystals were recrystallized from a 1:3 (vol.) ethyl acetate–cyclohexane mixture. Small white needles were recovered, dried under vacuum, and weighed. Small white needles were recovered, dried under vacuum, and weighted. The yield is 65% (60.8 g) based on methanedisulfonic acid. The HPLC purity was 99.5%, ^1H NMR (CD3CN, 400 MHz, ppm): δ 5.980 (s, 2H); 5.307 (s, 2H). ^{13}C NMR (CD3CN, 400 MHz, ppm): δ 91.94; 69.94. The residual metal ions were detected by ICP method, the result (ppm) was: Fe, 10.65; Ca, 7.46; Na, 19.22; K, 22.40.

2.2. Preparation of electrolyte and electrode

The electrolyte of 1.0 M $LiPF_6$-EC/DMC/EMC(1:1:1, wt.%) was purchased from Zhangjiagang Guotai-Huarong New Chemical Materials Co., Ltd., China. The electrolytes of 1.0 M $LiPF_6$-EC/DMC/EMC (1:1:1, wt.%) with and without 0.5 wt.% MMDS additive were prepared in an argon-filled glove box, in which the oxygen and water content were less than 20 ppm. $LiMn_2O_4$ cathode materials were purchased from Citic Guoan Mengguli Source Technology Co., Ltd., China. The $LiMn_2O_4$ electrodes were prepared by mixing the $LiMn_2O_4$ powder (80 wt.%), carbon black (10 wt.%) and poly(-vinylidene fluoride) (PVDF 10 wt.%) in N-methylpyrrolidone (NMP) solvent. The mixed slurry was coated onto aluminum foil and dried at 120 °C at 12 h. The dried electrode was then compressed by a roller to make a compact and smooth film structure at room temperature. The electrode disks were then punched out of the coated foil sheets and weighted. $LiMn_2O_4$/Li cells were fabricated with 2025-coin type cells in the argon-filled glove box using Celgard 2325 as the separator.

2.3. Measurements

The charge–discharge behavior of the cells was tested on Land CT2001A tester (Wuhan, China). The cells were cycled firstly at 0.1 C three times, 0.2 C three times, 0.5 C three times, 1.0 C three times at 25 °C, they were cycled under constant current conditions over the range of 3.0–4.3 V. And then they were cycled at 1.0 C at 25 °C and 55 °C for cycling performance test, respectively.

The impedance of the cells after formation and 200 cycles at 55 °C were determined with CHI660D (Shanghai, China). The frequency was varied from 100 kHz to 10 mHz and the amplitude was set at 5 mV. The impedance data were analyzed using ZSimpWin Version 3.1 software.

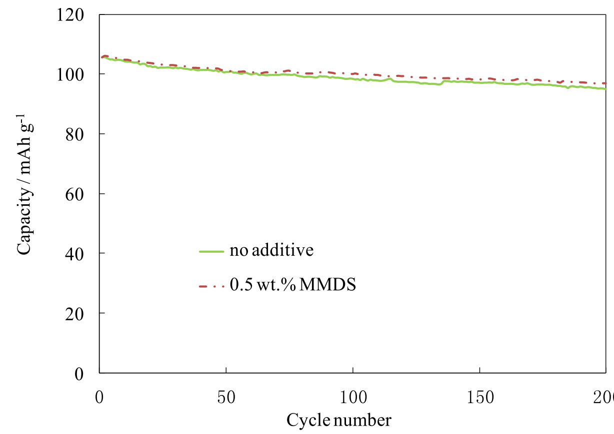

Fig. 1. Cycle performance of $LiMn_2O_4$/Li cell using 1 M $LiPF_6$ in EC/DMC/EMC (1:1:1, wt.%) as electrolytes with and without 0.5 wt.% MMDS additive at 25 °C. Charge–discharge rate was 1.0 C in the potential range of 3.0–4.3 V.

To analyze the composition and microstructure of the electrodes after charge–discharge cycling measurements, the cells were disassembled in a glove box under Ar atmosphere. The $LiMn_2O_4$ electrodes were washed with DMC solvent 5 times to remove residual electrolytes followed by vacuum drying for 12 h at room temperature. Scanning electron microscope (SEM, JSM-6700F, JEOL) and transmission electron microscope (TEM JEM-2010, JEOL) were used to investigate the morphology of the electrodes. The chemical composition of the surface layer on the $LiMn_2O_4$ was analyzed by X-ray photoelectron spectroscopy (XPS, ESCALAB 250, Thermo Scientific) with Al Ka line as an X-ray source. Binding energies were calibrated by using the containment carbon (C1s = 284.6 eV).

3. Results and discussion

The $LiMn_2O_4$/Li cells were assembled containing 1.0 M $LiPF_6$-EC/DMC/EMC (1:1:1, wt.%) electrolytes without and with the presence of 0.5 wt.% MMDS additive. The cells were cycled at 1.0 C under constant current conditions. The experiments were carried out at

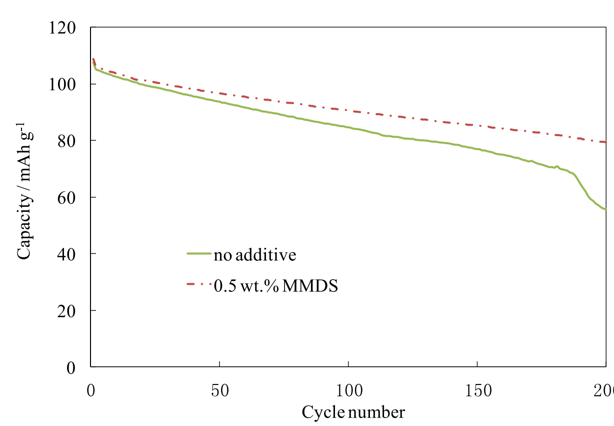

Fig. 2. Cycle performance of $LiMn_2O_4$/Li cell using 1 M $LiPF_6$ in EC/DMC/EMC (1:1:1, wt.%) as electrolytes with and without 0.5 wt.% MMDS additive at 55 °C. Charge–discharge rate was 1.0 C in the potential range of 3.0–4.3 V.

25 °C and 55 °C. Fig. 1 shows the cycle performance of the $LiMn_2O_4$/Li cells at 25 °C with different electrolytes. The cell with the electrolyte without MMDS displayed about 10.2% capacity loss at the 200th cycle, while the cell containing 0.5 wt.% MMDS additive showed only 8.2% capacity loss at the same cycle number. The results confirm that the addition of MMDS does not affect significantly the performance of the cells cycled at 25 °C.

Fig. 2 shows the cycle performance of the $LiMn_2O_4$/Li cells at 55 °C with different electrolytes. It is clearly found that capacity of the cell without additive faded more quickly than that the cell containing MMDS additive. The cell with the electrolyte without MMDS displayed about 21.4% capacity loss at the 100th cycle and 48.4% capacity loss at the 200th cycle, while the cell containing 0.5 wt.% MMDS additive showed only 16.8% capacity loss at the 100th cycle and 27.2% capacity loss at the same cycle number. MMDS improves the capacity retention at 55 °C.

The charge–discharge profiles of the $LiMn_2O_4$/Li cells cycled at 25 °C and 55 °C are shown in Figs. 3 and 4, respectively. It could be found that the charge–discharge profiles of the cells with the different electrolytes show nearly same at 25 °C. Compared with the cell cycled at 25 °C, there were significant changes of the discharge profiles of the cells cycled at 55 °C. The change of charge–discharge platform of the cell without additive was larger than the cell containing MMDS additive (Fig. 4). Unlike the cell with the electrolyte without additive, the cell with the electrolyte containing 0.5 wt.% MMDS additive exhibited negligible polarization and smooth charge–discharge profiles.

Fig. 5 presents the impedance measurement results of the $LiMn_2O_4$/Li cells with different electrolytes. The impedance was measured after the cells were full charged. The typical EIS of the Li-ion cells is composed of two partially overlapped semicircles and

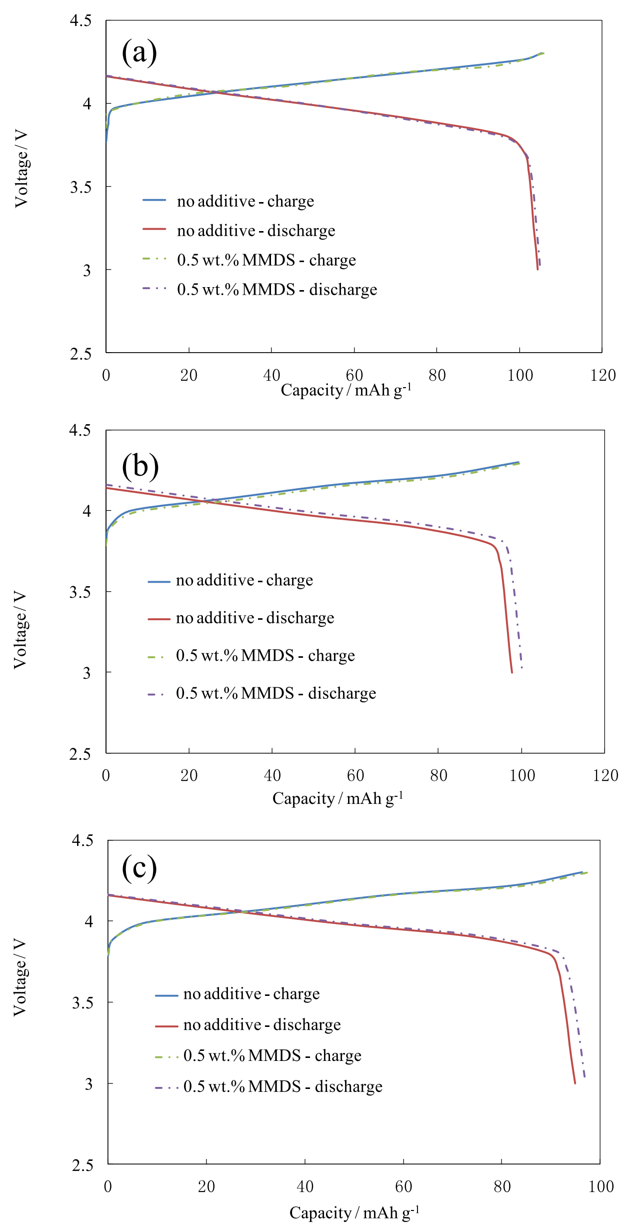

Fig. 3. Charge–discharge curve performance of $LiMn_2O_4$/Li cell using 1 M $LiPF_6$ in EC/DMC/EMC (1:1:1, wt.%) as electrolytes with and without 0.5 wt.% MMDS additive at 25 °C: (a) 10th cycle; (b) 100th cycle; (c) 200th cycle.

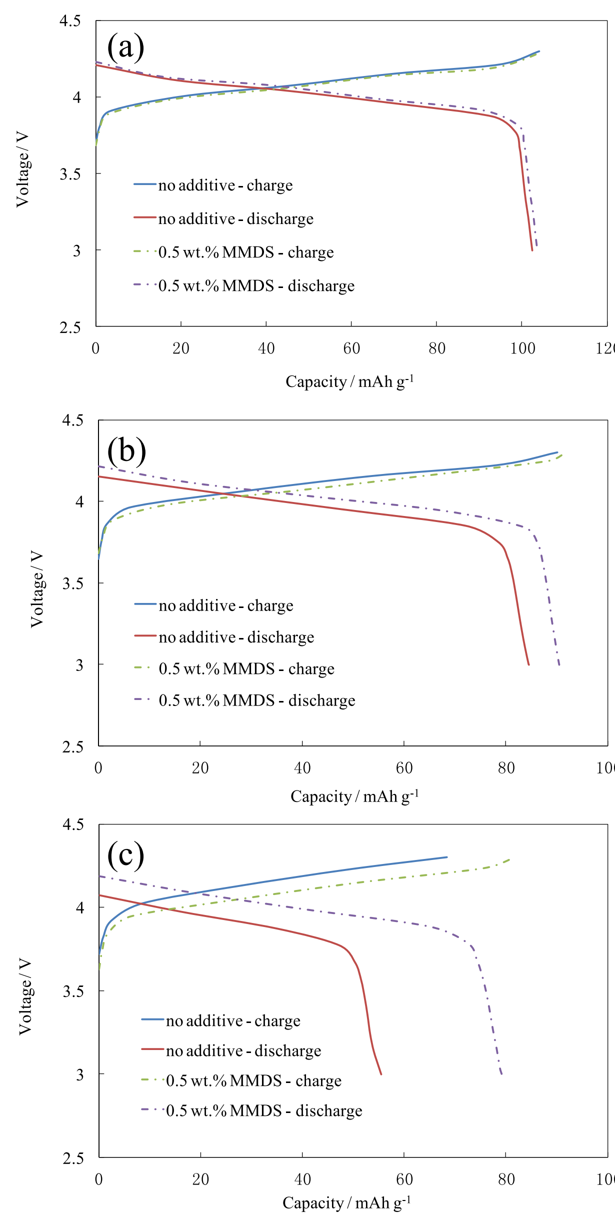

Fig. 4. Charge–discharge curve performance of $LiMn_2O_4$/Li cell using 1M $LiPF_6$ in EC/DMC/EMC (1:1:1, wt.%) as electrolytes with and without 0.5 wt.% MMDS additive at 55 °C: (a) 10th cycle; (b) 100th cycle; (c) 200th cycle.

a straight slopping line at low frequency end [15–20]. The R_e is bulk resistance of the cell, which reflects electric conductivity of the electrolyte, separator, and electrodes; R_f and C_f are resistance and capacitance of the solid-state interface layer formed on the surface of the electrodes, which correspond to the semicircle at high frequencies; R_{ct} and C_{dl} are faradic charge-transfer resistance and its relative double-layer capacitance, which correspond to the semicircle at medium frequencies; W is the Warburg impedance arising from the semi-infinite diffusion of Li^+ ions in $LiMn_2O_4$ electrode. Using the above-described model and ZSimpWin software, individual values of R_e, R_f, R_{ct} were obtained through fitting. The fitted impedance values obtained are shown in Table 1. The interfacial impedances of the cells after the formation cycle at 25 °C with and without MMDS additive are 23.98 Ω and 19.06 Ω, respectively. It indicates that the R_f with different electrolytes are nearly same after the formation cycle at 25 °C. After 200 cycles at 55 °C, the R_f of the cell with MMDS (31.08 Ω) was a bit smaller than the cell without additive (44.92 Ω). And the R_{ct} of the cells after the formation cycle at 25 °C with and without MMDS additive are 26.79 Ω and 31.94 Ω, respectively. However, after 200 cycles at 55 °C, the R_{ct} of the cell with MMDS (58.89 Ω) was a significant smaller than the cell without additive (390.8 Ω). The similar behaviors were also found in the $LiCoO_2$/graphite cell [14]. Li^+ migration through the surface film is prompted by the MMDS decomposed products. It assumed that an ionic conductive film can be formed on the $LiMn_2O_4$ surface due to MMDS additive, which is helpful for the intercalation of Li^+ to the $LiMn_2O_4$ particles, and thus improves the cycling performance.

To further investigate the effect of the MMDS on the $LiMn_2O_4$ electrode at elevated temperature, surface analysis of the electrodes was obtained after the cycling test of the coin cells. Fig. 6 shows SEM micrographs of a pristine $LiMn_2O_4$ electrode and the electrodes after cycled with the different electrolytes at 55 °C. From the SEM measurements it can be found that there were $LiMn_2O_4$ particles with an average size of a few μm and nano-sized conductive carbon into the pristine $LiMn_2O_4$ electrode. Compared to the pristine $LiMn_2O_4$ electrode (Fig. 6(a,b)), it can be found that the morphology of the $LiMn_2O_4$ electrodes without MMDS after 200 cycles at 55 °C shows a significant change (Fig. 6(c,d)). There are some fluff-like substances covered onto the surface of the electrode. These substances on the electrode surface may be a kind of SEI which was produced from electrolyte decomposition on the electrode surface, forming thick residue films. The morphology of the $LiMn_2O_4$ electrode with MMDS after 200 cycles at 55 °C (Fig. 6(e,f)) appears similar to the morphology of the pristine electrode, it indicates that MMDS would effectively prevented the erosion to $LiMn_2O_4$ of the electrolyte, which resulted in improving performance of the cells.

Fig. 7 shows TEM micrographs of a pristine $LiMn_2O_4$ electrode and the electrodes after cycled with the different electrolytes at 55 °C. From Fig. 7(a), a clear boundary can be observed on the pristine $LiMn_2O_4$ electrode. Whereas, there are some substances covered onto the surface of the cathode after 200 cycles, which are known to be SEI, as shown in Fig. 7(b, c). It can be found that the SEI derived from the electrolyte containing MMDS shows a layer with a thickness approximately 1–2 nm, which is thinner than that derived from the electrolyte without additive (with a thickness about 6–10 nm). This thinner surface film would decrease the interfacial resistance of cell.

The surfaces of the $LiMn_2O_4$ electrodes after 200 cycles at 55 °C with the different electrolytes were analyzed by XPS. The F 1s, O 1s, S 2p spectra of the $LiMn_2O_4$ electrodes are shown in Fig. 8. In the F 1s spectra, it could be found that the intensity of LiF (684.5 eV [20,21]) of the $LiMn_2O_4$ electrode without additive is much stronger than that with MMDS additive. And in the O 1s spectra, the intensities of Li_2CO_3 (532.0 eV [20]) observed on the surface of the $LiMn_2O_4$ electrode without additive are stronger than that with 0.5 wt.% MMDS. It indicated more LiF, Li_2CO_3 was covered on the $LiMn_2O_4$ electrode with the conventional electrolyte. The intensities of C=O (531.3 eV [20,22]) bonds observed on the surface of the $LiMn_2O_4$ electrode with 0.5 wt.% MMDS are stronger than that without additive, while the intensities of C–O (533.3 eV [20,22]) bonds observed on the surface of the $LiMn_2O_4$ electrode without additive are stronger than that with 0.5 wt.% MMDS, it means that MMDS can hinder the polymerization of EC solvent efficiently [20,22].

To further confirm the fact that MMDS participated in the formation of SEI on the surface of the $LiMn_2O_4$ electrode, S 2p spectra of the electrode with MMDS additives were measured. In the S 2p spectra, two peaks can be observed, the peaks at 169.1 eV [23] and 167.9 eV [23] are assigned to Li_2SO_3 and $ROSO_2Li$. These results indicate that the MMDS additives participated in the formation of SEI. The possible reaction paths of MMDS are presented in Fig. 9. It is similar to that of PES [23] and PS [24]. A radical anion coordinated with lithium ion (a) is formed at the first step of the reduction of

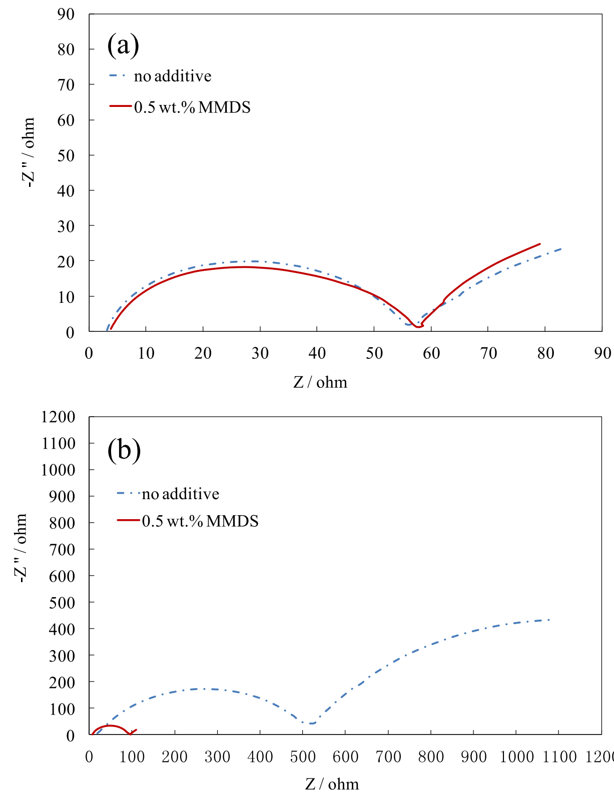

Fig. 5. Electrochemical impedance spectra of $LiMn_2O_4$/Li cell with and without 0.5 wt.% MMDS after (a) formation at 25 °C; (b) 200 cycles at 55 °C

Table 1
Impedance parameters of $LiMn_2O_4$ electrode in electrolyte with and without 0.5 wt.% MMDS additive after formation at 25 °C and after 200 cycles at 55 °C.

Electrolyte	R_e/ Ω	R_f/ Ω	C_f/ μF	R_{ct}/ Ω	C_{dl}/ μF
No additive after formation at 25 °C	3.446	19.06	3.235	31.94	9.492
After 200 cycles at 55 °C	21.47	44.92	1.248	390.8	3.041
0.5 wt.% MMDS after formation at 25 °C	4.241	23.98	2.342	26.79	1.346
After 200 cycles at 55 °C	8.247	31.08	2.193	58.89	6.482

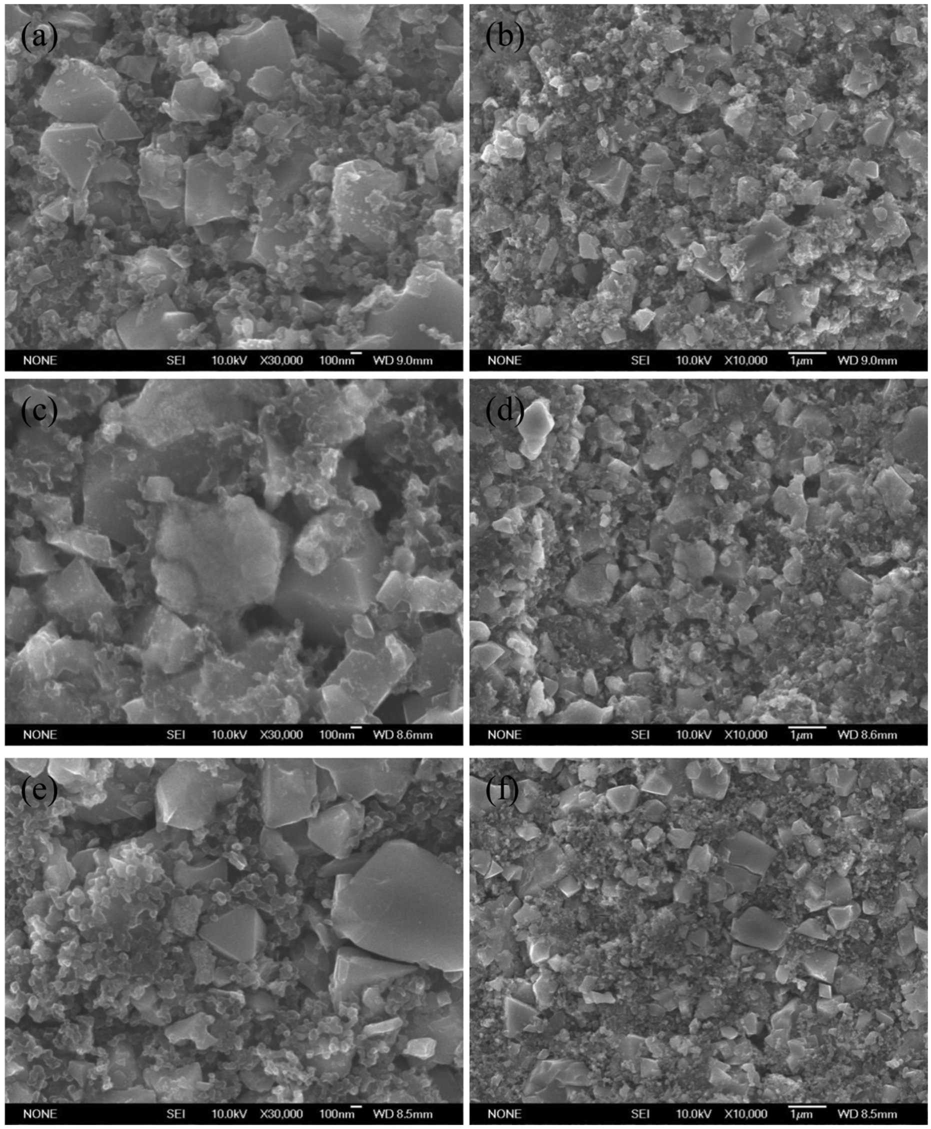

Fig. 6. SEM micrographs of $LiMn_2O_4$ electrodes: pristine electrode (a) 30,000× (b) 10,000×, and electrodes after 200 cycles at 55 °C using 1 M $LiPF_6$ in EC/DMC/EMC (1:1:1, wt.%) as electrolytes without (c) 30,000× (d) 10,000× and with 0.5 wt.% MMDS additive (e) 30,000× (f) 10,000×.

MMDS with one electron transfer, followed by the formation of radical alkyl sulfonate (b) with another electron transfer. Intermediate (b) could further decompose into Li_2SO_3 and alkyl sulfonate (c), and intermediate (c) could further reduced to radical alkyl sulfonate (d). Several products may be formed from the radical alkyl sulfonate (d), for example, (i) the formation of Li_2SO_3 and ethylene (e) due to the reaction with Li^+; (ii) the formation of alkyl sulfonate (f), when (d) is reduced with a one electron transfer accompanying the formation of the C=C bond; (iii) the formation of alkyl sulfonate (g), R may be C_2H_5 in (g) when (d) is reduced with a one electron transfer and without the formation of the C=C bond, or R may be CH_3 in (g) when (d) takes place with two electron transfer accompanying the breakdown of a C–C bond; (iv) the formation of dimer (h) due to the self-dimerization of (d).

As discussed above, it can be found that more inorganic degradation products such as Li_2CO_3 and LiF were covered on the $LiMn_2O_4$ electrode with the conventional electrolyte compared with the electrode containing the MMDS additive. It is well known that the LiF is a nonconductor for both electrons and lithium ions, hence the formed LiF onto the electrodes will result in increasing the interfacial impedance of the cells, which consistent with the results of Table 1. Therefore, the dissolution of the LiF from the passivation film can result in lower interfacial impedance. In addition, $ROSO_2Li$ was formed on the surface of the $LiMn_2O_4$ electrode, which will also improve the transportation of Li^+. Based on these effects, it results in the cell resistance in the electrolyte containing the MMDS additive was smaller than that with the conventional electrolyte.

4. Conclusions

It has been proved that the MMDS can be used as an effective electrolyte additive for formation of a good SEI layer on the $LiMn_2O_4$ electrode at elevated temperature. The stable SEI layer derived from MMDS, becomes thinner and shows a reduction in interfacial resistance and a good ability of Li^+ migration, which leads to the improvement of cycling performance of the cell especially at high temperature.

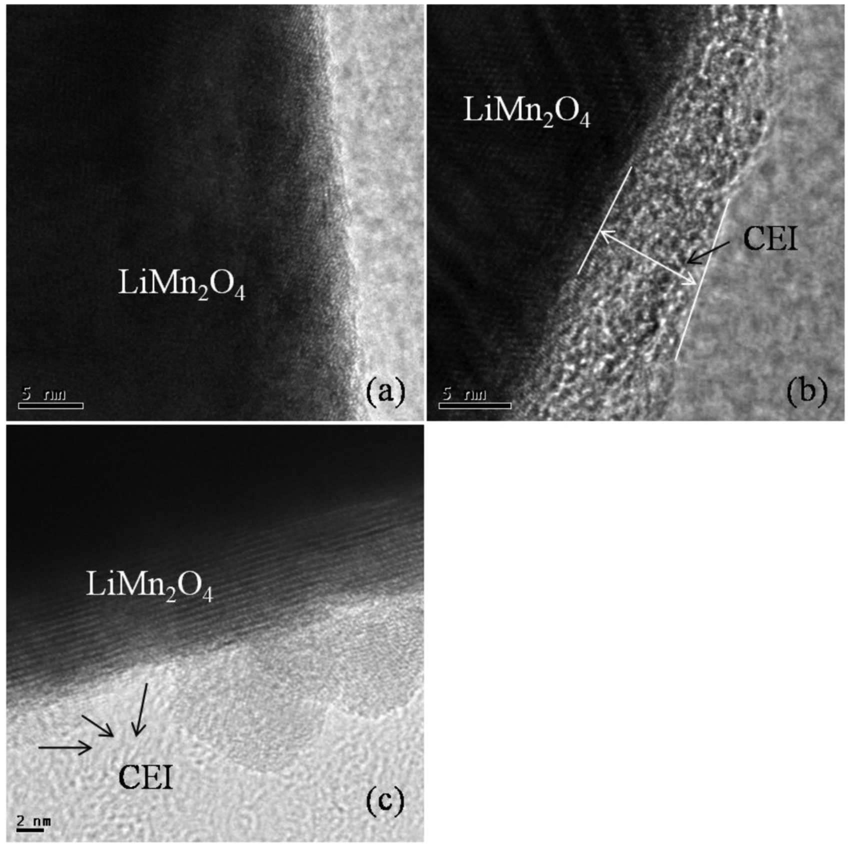

Fig. 7. TEM micrographs of $LiMn_2O_4$ electrodes: (a) pristine electrode, and electrodes after 200 cycles at 55 °C using 1 M $LiPF_6$ in EC/DMC/EMC (1:1:1, wt.%) as electrolytes (b) without additive and (c) with 0.5 wt.% MMDS additive.

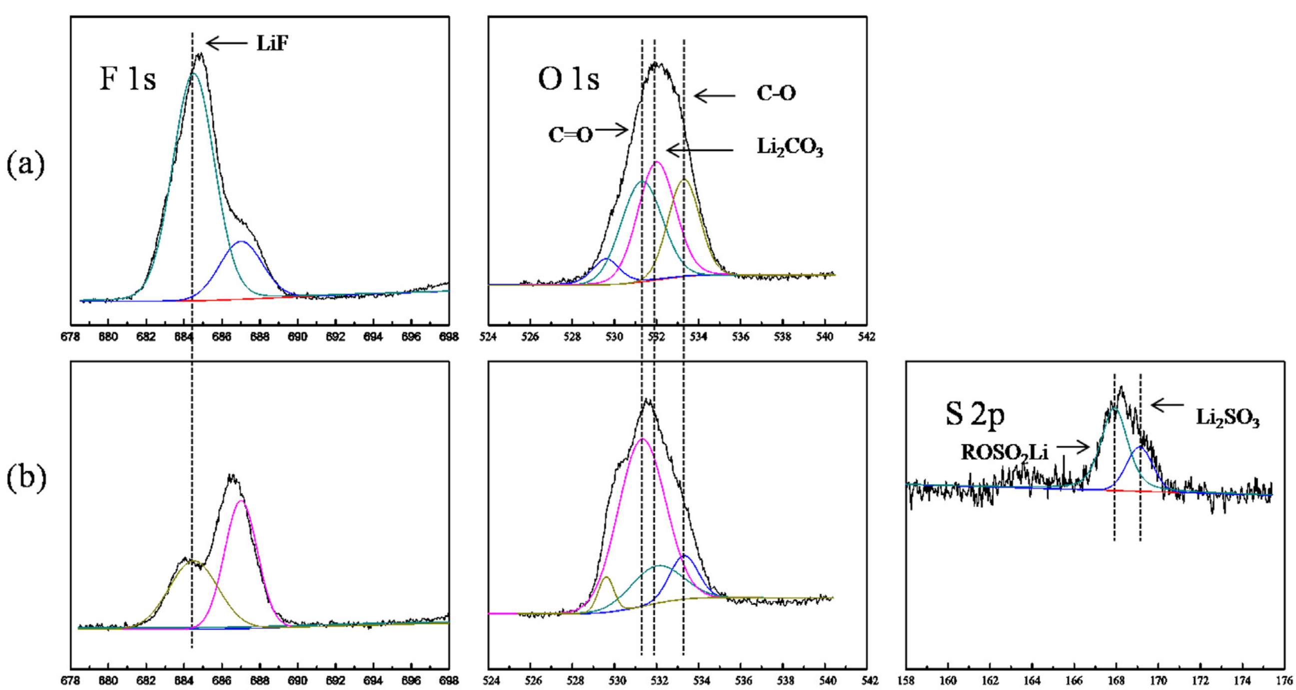

Fig. 8. The F 1s, O 1s and S 2p XPS spectra of $LiMn_2O_4$ electrodes after 200 cycles at 55 °C using 1 M $LiPF_6$ in EC/DMC/EMC (1:1:1, wt.%) as electrolytes (a) without additive and (b) with 0.5 wt.% MMDS.

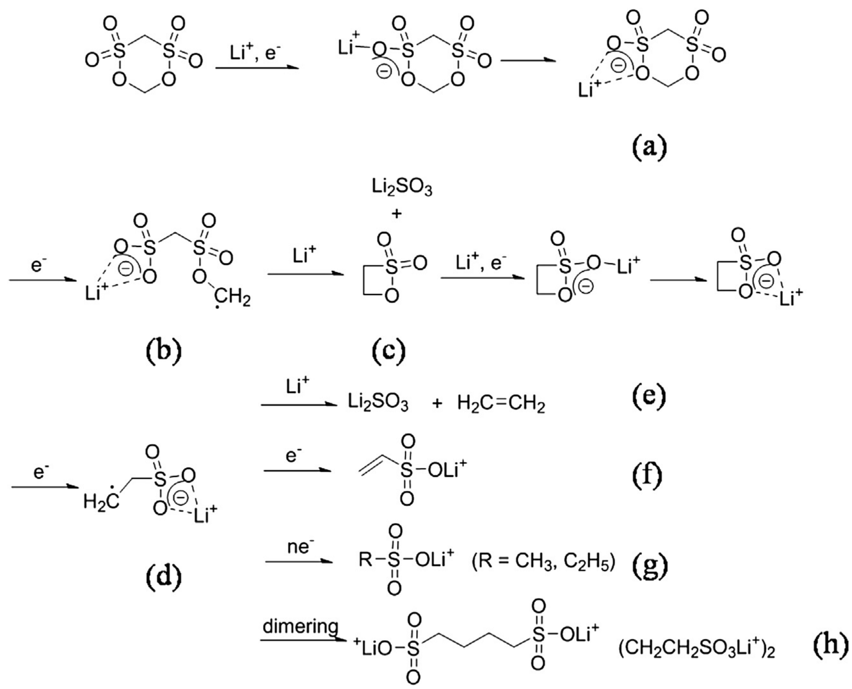

Fig. 9. Possible reaction paths of MMDS on $LiMn_2O_4$ electrodes in 1.0 M $LiPF_6$-EC/DMC/EMC (1:1:1, wt.%) with 0.5 wt.% MMDS.

Acknowledgments

This work was supported by the "Strategic Priority Research Program" of the Chinese Academy of Sciences, Grant No. XDA09010103, FIPYT (No. 2013H20003-1) and 973 program 2011CBA00507, 2011CB935904.

References

[1] D.K. Kim, P. Murralidharan, H.W. Lee, R. Ruffo, Y. Yang, C.K. Chan, H. Peng, R.A. Huggins, Y. Cui, Nano Lett. 8 (2008) 3948.
[2] H.W. Lee, P. Muralidharan, R. Ruffo, C.M. Mari, Y. Cui, D.K. Kim, Nano Lett. 10 (2010) 3852.
[3] Y.Y. Xia, T. Sakai, T. Fujieda, X.Q. Yang, X. Sun, Z.F. Ma, J. McBreen, M. Yoshio, J. Electrochem. Soc. 148 (2001) A723.
[4] M. Wohlfahrt-Mehrens, C. Vogler, J. Garche, J. Power Sources 127 (2004) 58.
[5] H. Yamane, M. Saitoh, M. Sano, M. Fujita, M. Sakata, M. Takada, E. Nishibori, N. Tanaka, J. Electrochem. Soc. 149 (2002) A1514.
[6] L. Yang, M. Takahashi, B.F. Wang, Electrochim. Acta 51 (2006) 3228.
[7] J.B. Goodenough, J. Power Sources 174 (2007) 996.
[8] Y.L. Dai, L. Cai, R.E. White, J. Electrochem. Soc. 160 (2013) A182.
[9] S.S. Zhang, J. Power Sources 162 (2006) 1379.
[10] X. Sun, H.S. Lee, X.Q. Yang, J. McBreen, Electrochem. Solid-State Lett. 5 (2002) A248.
[11] M.H. Ryou, G.B. Han, Y.M. Lee, J.N. Lee, D.J. Lee, Y.O. Yoon, J.K. Park, Electrochim. Acta 55 (2010) 2073.
[12] Y.K. Li, R.X. Zhang, J.S. Liu, C.W. Yang, J. Power Sources 189 (2009) 685.
[13] Y.B. Liu, L. Tan, L. Li, J. Power Sources 221 (2013) 90.
[14] X.X. Zuo, C.J. Fan, X. Xiao, J.S. Liu, J.M. Nan, J. Power Sources 219 (2012) 94.
[15] D. Aurbach, K. Gamolsky, B. Markovsky, G. Salitra, Y. Gofer, U. Heider, R. Oesten, M. Schmidt, J. Electrochem. Soc. 147 (2000) 1322.
[16] S.S. Zhang, K. Xu, T.R. Jow, J. Electrochem. Soc. 149 (2002) A1521.
[17] M. Mohamedi, D. Takahashi, T. Itoh, I. Uchida, Electrochim. Acta 47 (2002) 3483.
[18] T.H. Nam, E.G. Shim, J.G. Kim, H.S. Kim, S.I. Moon, J. Power Sources 180 (2008) 561.
[19] C.J. Curtis, J.X. Wang, D.L. Schulz, J. Electrochem. Soc. 151 (2004) A590.
[20] K.A. Striebel, E. Sakai, E.J. Cairns, J. Electrochem. Soc. 149 (2002) A61.
[21] D. Chalasani, J. Li, N.M. Jackson, M. Payne, B.L. Lucht, J. Power Sources 208 (2012) 67.
[22] L. Yang, B. Ravdel, B.L. Lucht, Electrochem. Solid-State Lett. 13 (2010) A95.
[23] B. Li, M.Q. Xu, B.Z. Li, Y.L. Liu, L. Yang, W.S. Li, S.J. Hu, Electrochim. Acta 105 (2013) 1.
[24] X.X. Zuo, M.Q. Xu, W.S. Li, D.G. Su, J.S. Liu, Electrochem. Solid-State Lett. 9 (2006) A196.